

# Estimating glacier snow accumulation from backward calculation of melt and snowline tracking

John HULTH,<sup>1</sup> Cecilie ROLSTAD DENBY,<sup>1</sup> Regine HOCK<sup>2,3</sup>

<sup>1</sup>*Department of Mathematical Sciences and Technology, Norwegian University of Life Sciences, Ås, Norway  
E-mail: cecilie.rolstad@umb.no*

<sup>2</sup>*Geophysical Institute, University of Alaska Fairbanks, Fairbanks, USA*

<sup>3</sup>*Department of Earth Sciences, Uppsala University, Uppsala, Sweden*

**ABSTRACT.** Estimating precipitation to determine accumulation is challenging. We present a method that combines melt modelling and snowline tracking to determine winter glacier snow accumulation along snowlines. The method assumes that the net accumulation is zero on the transient snowlines and the maximum winter accumulation at the snowline can be calculated backwards with a temperature-index melt model. To verify the method, the accumulation model is applied for the year 2004 on Storglaciären, Sweden, for which extensive meteorological and mass-balance data are available. The measured mean snowline accumulation is  $0.94 \pm 0.10$  m w.e. for 2004. Modelled accumulation, using backward melt modelling, at the same snowlines is  $0.82 \pm 0.25$  m w.e. The accumulation model is also compared with an often used linear regression accumulation model which yields a mean snowline accumulation of  $1.02 \pm 0.38$  m w.e. The reduction in standard error from 0.38 m w.e. to 0.25 m w.e. shows that the backward melt modelling applied at snowlines can provide a better spatial representation of the accumulation pattern than the regression model. Importantly, the applied method requires no field measurements of accumulation during the winter and snowlines can be readily traced in remotely sensed images.

## INTRODUCTION

Glacier mass-balance modelling can be divided into accumulation and melt modelling. Both of these require accurate meteorological input data (e.g. precipitation and temperature). An essential problem in mass-balance modelling is the lack of available and accurate meteorological data. Small-scale meteorological conditions affecting snowfall in mountainous areas tend to vary significantly in both space and time, and point measurements on rocks or stations near glaciers may not be suitable for extrapolation to the glacier surface of interest. Air temperature, which is an important input variable for modelling, is easier to extrapolate over glacierized areas. By using assumptions concerning lapse rates and extrapolation techniques (e.g. Gardner and Sharp, 2009) it is possible to determine temperature fields to a higher degree of accuracy than precipitation.

Snow-depth observations and melt modelling have been used successfully to determine the snow water equivalent accumulation in previous studies in mountain areas (Rango and Martinec, 1982; Bagchi, 1983; Cline, 1997; Raleigh and Lundquist, 2009, 2010). Others have used the snow depletion as validation of different mass-balance models (Blöschl and others, 1991; Farinotti and others, 2010). In this paper we explore a method that establishes an indirect relationship between temperature and peak accumulation (winter mass balance). We show that it is possible to estimate the winter accumulation from observed snow depletion data within the same accuracy range as for modelled summer melt. The input data needed are information on the snow-cover extent for one or multiple time-steps during the following melt season and air temperature. A required model parameter in the temperature-index melt model is a calibrated melt factor of snow. Calibration of the melt factor requires ablation stakes and snow density measurements. Transient snowlines can be

used to improve the spatial distribution of the accumulation. Snowlines are readily detected in satellite images and aerial photographs and can be digitized with high precision (Williams and others, 1991; Turpin and others, 1997) or they can be measured on the glacier.

The method of backward melt modelling, referred to here as 'accumulation modelling', is applied to an extensive meteorological and mass-balance dataset from Storglaciären, Sweden, for the year 2004. In this year transient snowlines were measured in the field using GPS on several occasions (Kootstra, 2005; Hock and others, 2007) and extensive probing and stake measurements were also carried out. Such data are only available for the year 2004. In addition, we have chosen this glacier for a number of other significant reasons: (1) there is an extensive mass-balance dataset for the glacier (Holmlund and Jansson, 1999; Holmlund and others, 2005; Zemp and others, 2010); (2) hourly temperature and precipitation data are available from the nearby Tarfala Research Station (Grudd and Schneider, 1996); (3) temperature-index modelling of the glacier has been conducted previously (Hock, 1999); and (4) the accumulation is highly influenced by the topography (Hulth, 2006).

The relation between air temperature and glacier melt (Ohmura, 2001; Sicart and others, 2005) has been used successfully to develop melt models based on a simple parameterization. Topographic features and solar geometry have been included to further enhance the classical temperature-index methods (e.g. Hock, 1999; Pellicciotti and others, 2005). Hock's well-established temperature-index model is applied in this study.

Regression analysis, usually least-squares fitting of linear models, is also commonly used in mass-balance models to determine accumulation and it is of interest to determine whether the backwards melt modelling approach used here improves the results. A linear least-squares regression

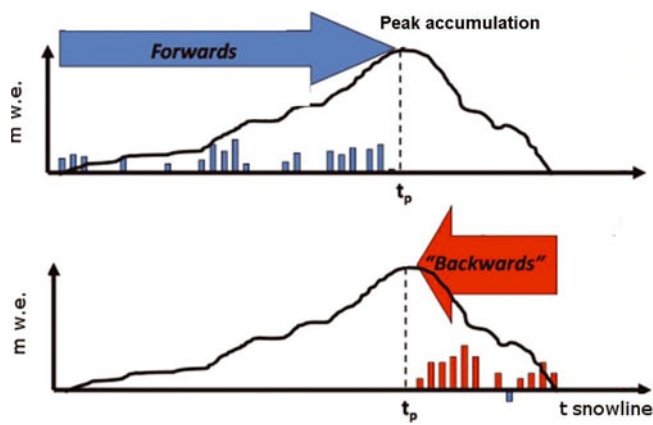


**Fig. 1.** Illustration of the accumulation model. Vertical axis is calculated melt or accumulation (m.w.e.). Horizontal axis is time, with peak accumulation at  $t_p$  and the timing of the snowline,  $t_{\text{snowline}}$ , marked. Blue bars illustrate precipitation events and red bars show melt events. Positive bars indicate the direction of integration (forwards or backwards). Adapted from Raleigh and Lundquist (2009).

analysis on measured snow accumulation with elevation (87 mass-balance stakes) is conducted here and the results from both the accumulation model and the linear regression model are compared. Both methods are compared with the measured snow accumulation derived from kriging on 266 snow-probing points, measured independently of the 87 mass-balance stakes.

## ACCUMULATION MODEL

The accumulation model is based on the principle that it is easier to model melt spatially during the summer than to determine accumulation during the winter. Ablation is strongly related to positive air temperature and potential incoming solar radiation. Melt has been modelled previously on Storglaciären with an enhanced temperature-index model with good results (Hock, 1999). Accumulation on the other hand is highly influenced by the local meteorology and the topography since the snow is redistributed by wind after snowfall. Therefore it is difficult to model accumulation with a simple parameterization and it requires dense meteorology observations as input.

The accumulation is estimated using backwards calculations of the melt, applying a temperature-index model (Fig. 1). At the snowline location all snow from the previous winter has melted, while the ice melt has not yet started. If superimposed ice is insignificant, the snowline therefore corresponds to zero net mass balance. The total melt at a snowline from the beginning of the melt season to the snowline observation is calculated using the temperature-index model, and the result represents the peak winter accumulation along the snowline.

The melt for the accumulation model is calculated applying a temperature-index model. Traditional models rely on a linear relation between melt and positive air temperature and are a good measure of average glacier melt. However, these models are restricted both spatially and temporally. Topographic effects such as surface slope, aspect and topographic shading introduce variation in melt rates. Therefore, we have chosen a temperature-index model that includes potential clear-sky radiation, which can be

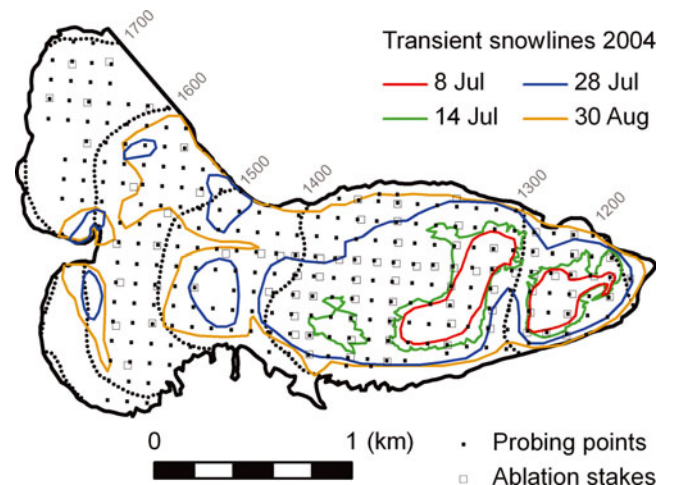


**Fig. 2.** Data for Storglaciären, 2004. Coloured lines indicate observed snowlines at the four different dates, and black dotted lines are elevation contours. Black dots show the 266 snow-probing points and grey squares the 87 ablation stakes.

calculated without any additional meteorological input data, while introducing a spatial and temporal distribution of the melt rate considering topographic effects (Hock, 1999). This model was developed for Storglaciären but is generally applicable to glaciers of different sizes and located in a wide range of climatic conditions (Hock and others, 2002; Schuler and others, 2005, 2007; Huss and others, 2007).

A complete description of the melt model is provided by Hock (1999). However, we provide some information here. Melt  $M$  ( $\text{mm h}^{-1}$ ) is calculated as

$$M = \begin{cases} \left(\frac{1}{n} M_{\text{factor}} + \alpha_{\text{snow}} I\right) T & : T \leq 0 \\ 0 & : T > 0 \end{cases} \quad (1)$$

where  $n$  is the number of time-steps per day,  $M_{\text{factor}}$  (called MF in Hock, 1999) is a melt factor ( $\text{mm d}^{-1} (\text{°C})^{-1}$ ),  $\alpha_{\text{snow}}$  ( $\text{m}^2 \text{W}^{-1} \text{mm h}^{-1} (\text{°C})^{-1}$ ) is a radiation coefficient for snow surfaces,  $I$  ( $\text{W m}^{-2}$ ) is potential clear-sky direct solar radiation at the snow surface and  $T$  ( $\text{°C}$ ) is air temperature. The calculation of the potential clear-sky radiation is described in Hock (1999), and through this term topographic effects such as slope, aspect and effective horizon and daily cycles of melt rates are included.

## DATA

Storglaciären (Fig. 2) is a polythermal glacier in northern Sweden at  $67^{\circ}54'10'' \text{N}$ ,  $18^{\circ}34'0'' \text{E}$ . The glacier is about 3.5 km long and covers an area of  $3.1 \text{ km}^2$  in the elevation range 1700–1150 m a.s.l.

Snowlines were tracked by walking along the line of transition of snow to ice on seven occasions between 8 July and 30 August 2004 (Table 1; Fig. 2). Measurements were conducted with a handheld GPS unit with a horizontal accuracy of about 10 m (Kootstra, 2005).

The winter snow accumulation was determined from 266 snow-probing points and snow density measurements at four pits conducted during two periods in spring 2004 (Kootstra, 2005). The ablation area, below 1450 m a.s.l., was measured from 18 to 25 April and the accumulation area, above 1450 m a.s.l., on 12 May (Table 1). The 266 snow-probing

**Table 1.** Measurement dates of snowlines, snow depth and ablation on Storglaciären, 2004

Day of year	Snowlines	Mass balance
108–115		18–25 April
		Snow-depth probing in ablation area (below 1450 m a.s.l.)
133		12 May
		Snow depth in accumulation area (above 1450 m a.s.l.) and stakes for entire glacier
190	8 July	8 July
196	14 July	
204	22 July	
210	28 July	
218	5 August	5 August
224	11 August	
243	30 August	
253		9 September
		Ablation

points were interpolated with regular kriging routines into a 30 m grid representing the snow accumulation of Storglaciären. The measured mean snow accumulation was  $0.94 \pm 0.10$  m w.e.

The heights above the glacier surface of 87 stakes for the whole glacier were also measured on 12 May, 8 July and 5 August to determine melt (see Table 1). Melt is thus determined for three periods in the summer.

We use a digital elevation model (DEM) of Storglaciären from 1990 (Holmlund, 1996) with a  $30 \text{ m} \times 30 \text{ m}$  grid spacing.

## APPLICATION

### Temperature-index melt model set-up

Melt is calculated by a temperature-index model on an hourly basis for each gridcell on the glacier. Potential snowmelt can be extracted for each time-step at the snowline corresponding to the previous winter's peak accumulation. For model simplicity the snowlines are represented on maps with equal grid size as the DEM, assuming that the mass balance does not vary significantly within a single gridcell ( $30 \text{ m} \times 30 \text{ m}$ ).

### Calibration of the melt model

Melt was measured at 87 ablation stakes several times during the melt season (Table 1), and the net mass balances are calculated for three periods of the ablation season to provide input data for calibration of the temperature-index melt model (Fig. 2). Assumptions concerning summer snow density evolution are taken from a previous study on Storglaciären by Kootstra (2005). Snow density was assumed to vary with time according to the snow density curve measured on Storglaciären by Schytt (1973), and this curve was used to assign snow densities to the dates when the stake measurements were carried out.

The model includes snow precipitation whenever the meteorological station records precipitation and the air temperature is below a threshold value of  $0.5^\circ\text{C}$ . A transition from solid to liquid precipitation mixture is used for the temperature interval  $0.5\text{--}2.5^\circ\text{C}$ , following Hock and Holmgren (2005). Air temperatures recorded at Tarfala Research

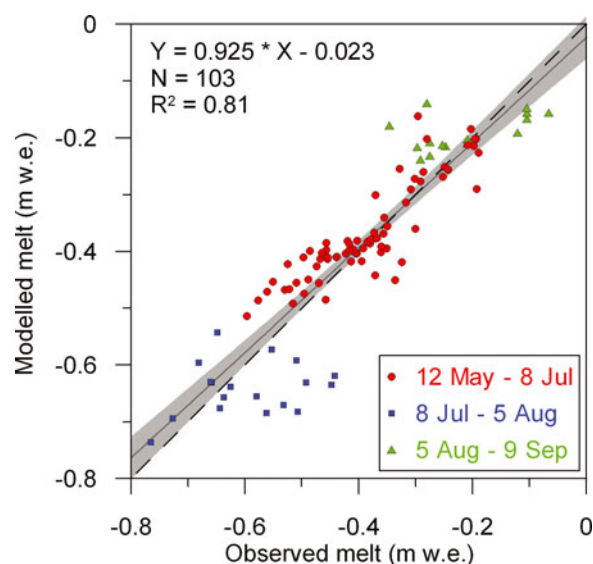


**Fig. 3.** Calibration of melt model: 87 mass-balance stakes of observed and modelled melt for calibration in three periods (blue: winter to 8 July; red: 8 July to 5 August; green: 5 August to 17 September). Not all stakes were visited in every measurement period. The dashed black line indicates the 1 : 1 line. The thin solid black line with associated grey area indicates a linear regression fit to these data points and its uncertainty.

Station (1130 m a.s.l.; Grudd and Schneider, 1996) were extrapolated using a lapse rate of  $0.58^\circ\text{C}(100 \text{ m})^{-1}$  which drives the model. Snow is distributed evenly over the glacier surface, taking into account the extrapolated air temperature.

Calibration of the temperature-index model was achieved by optimizing the efficiency criterion, as described in Nash and Sutcliffe (1970), between observed and simulated cumulative snowmelt during three sub-periods between 12 May and 9 September (Table 1; Fig. 3). Optimal agreement was achieved by varying the melt factor, the radiation factor for snow and the lapse rate (Hock, 1999). A melt factor of  $M_{\text{factor}} = 1.48 \text{ (mm d}^{-1} (\text{C}^\circ)^{-1})$ , a radiation factor of  $\alpha_{\text{snow}} = 0.30 \times 10^{-3} \text{ (m}^2 \text{W}^{-1} \text{ mm h}^{-1} (\text{C}^\circ)^{-1})$  and a lapse rate of  $0.58^\circ\text{C}(100 \text{ m})^{-1}$  gave the best agreement between observed and modelled cumulative melt for the entire period 12 May to 9 September. These optimal values are similar to those derived by Hock (1999) on the same glacier but for the year 1994. Figure 4 shows the sensitivity of the efficiency criteria, which is analogous to the coefficient of determination ( $R^2$ ), to variation in these parameters.

### Snow accumulation linear regression model

A snow accumulation gradient with elevation is derived using linear regression of observed accumulation with altitude at 87 mass-balance stakes (Fig. 5), independent of the 266 snow-probing points. The inclusion of surface slope, curvature and/or aspect did not improve the regression analysis.

## RESULTS: MODELLED ACCUMULATION

Observed and modelled accumulation along tracked snowlines is shown in Figure 6. Some measured snowlines have not been used for the assessment (at  $\sim 1600 \text{ m}$ ) as they lay outside the probing and stake network. As seen in Figure 6d and e, the accumulation model reproduces the spatial distribution of snow better than the regression model.

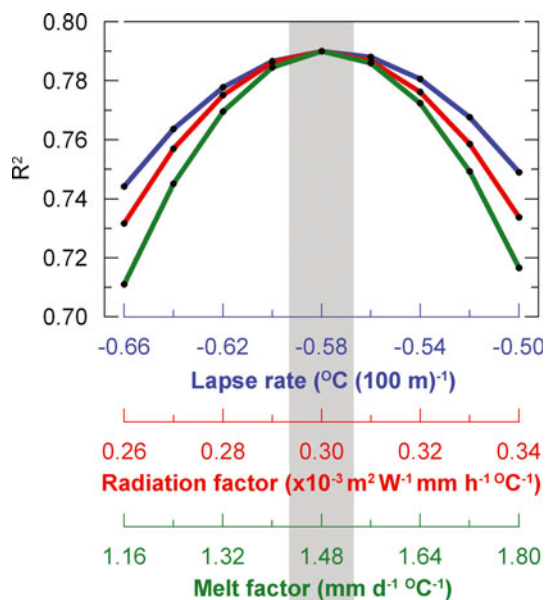


**Fig. 4.** Sensitivity of the efficiency criteria (coefficient of determination,  $R^2$ ) to the three model parameters used for the melt model calibration: lapse rate, radiation factor and melt factor. Optimal values are centred in the plot, indicated by the vertical grey bar.

The regression model tends to over-predict the accumulation above 1400 m while the accumulation model both under- and over-predicts in this area. The comparison with the observed winter accumulation also shows that the accumulation model reproduces the typical inhomogeneous snow distribution pattern of Storglaciären observed by Hulth (2006).

The accumulation model slightly underestimates the mean snowline accumulation by 10 cm w.e., and the regression analysis overestimates by 8 cm w.e. Standard deviation of the model residuals is significantly lower for the accumulation model than for the regression model, at 25 and 38 cm w.e., respectively. This is clear in the frequency distributions of the residuals (Fig. 7c and f).

## DISCUSSION

The uncertainties in the mean modelled winter accumulation relate primarily to the simplification of the physics in the temperature-index melt model; therefore, the modelled accumulation presented here will be at least as inaccurate as the results from the applied melt model. Uncertainties in snowline positions, presence of summer snowfalls and deviations from the assumption that the snowlines represent zero net balance also contribute to the total uncertainty in modelled winter accumulation. The contribution from the sum of these uncertainties in the snow accumulation modelling is assessed by comparison with observed data in this study.

In cases of summer snowfalls, the snowline position would move to a lower altitude on a subsequent date and the modelling concept would not be as applicable. Calculated melt would then be in periods of exposed ice instead of snow, which would lead to an incorrect calculation of accumulation. The presence of summer snowfall has to be considered through field observations or meteorological data when applying the method. For Storglaciären in summer 2004, when an extensive field campaign was conducted, the

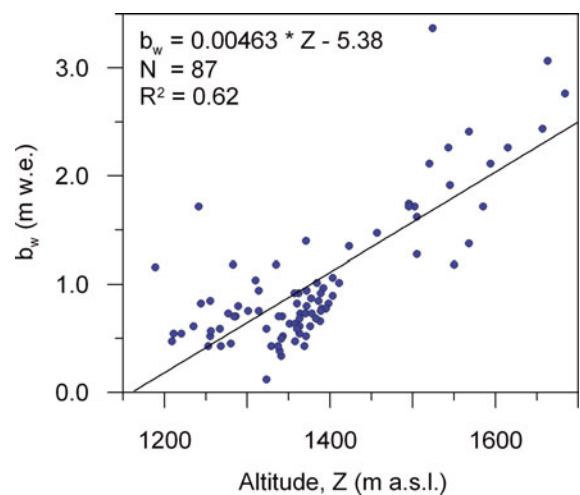


**Fig. 5.** Linear regression analysis of observed snow accumulation with elevation. The resulting fit is used to determine the linear regression accumulation model indicated in the figure. Measurements were carried out at 87 stakes on 12 May 2004.

first snowfalls were reported on 17 September 2004 (Kootstra, 2005), which is after our calculation period.

The calculated accumulation is compared with observed accumulation derived from the interpolation of 266 snow-probing points; however, there is an uncertainty connected to these snow accumulation grid values. The observed values are based on point measurements of snow depth converted to m w.e. using density measurements, thereafter distributed by interpolation and extrapolation to cover the entire glacier surface. Mean snowline accumulation error is expected to be about 10 cm w.e., but specific point values are likely to exceed the mean error by several times. This is primarily due to errors related to unprobed areas and inhomogeneous areas (e.g. crevassed areas) and, to some extent, variations not registered by the relatively sparse observations of snow density (Jansson, 1999). The comparison of the calculated mean snowline accumulations deviates from the observed by  $-0.12$  m w.e. for the accumulation model and 0.08 m w.e. for the regression model. This is within the range of the estimated uncertainty.

Hulth (2006) observed that the winter accumulation is highly influenced by topography. The linear regression analysis of the snow accumulation with elevation (Fig. 5) based on 87 mass-balance stakes yields a Pearson correlation coefficient of  $R^2 = 0.62$ , which is lower than the correlation of the melt model ( $R^2 = 0.81$ ) using the same set of stakes during the melt season. This shows that the accumulation pattern is not only a function of elevation, but may be dependent on other factors such as local topography and wind. As a result, the spatial distribution of snow accumulation cannot be estimated very well using linear regression, as shown by the regression results in Figure 6e. Including snowlines and melt modelling improves the spatial pattern of the modelled snow accumulation, as shown in Figure 6d. The standard deviation of the comparison of modelled versus observed is also reduced from 0.38 m w.e. to 0.25 m w.e. when applying the accumulation model at snowlines compared with the regression model, which shows that the spatial pattern of accumulation is better represented. The statistical results of the calibration and assessment of the model results are summarized in Table 2.

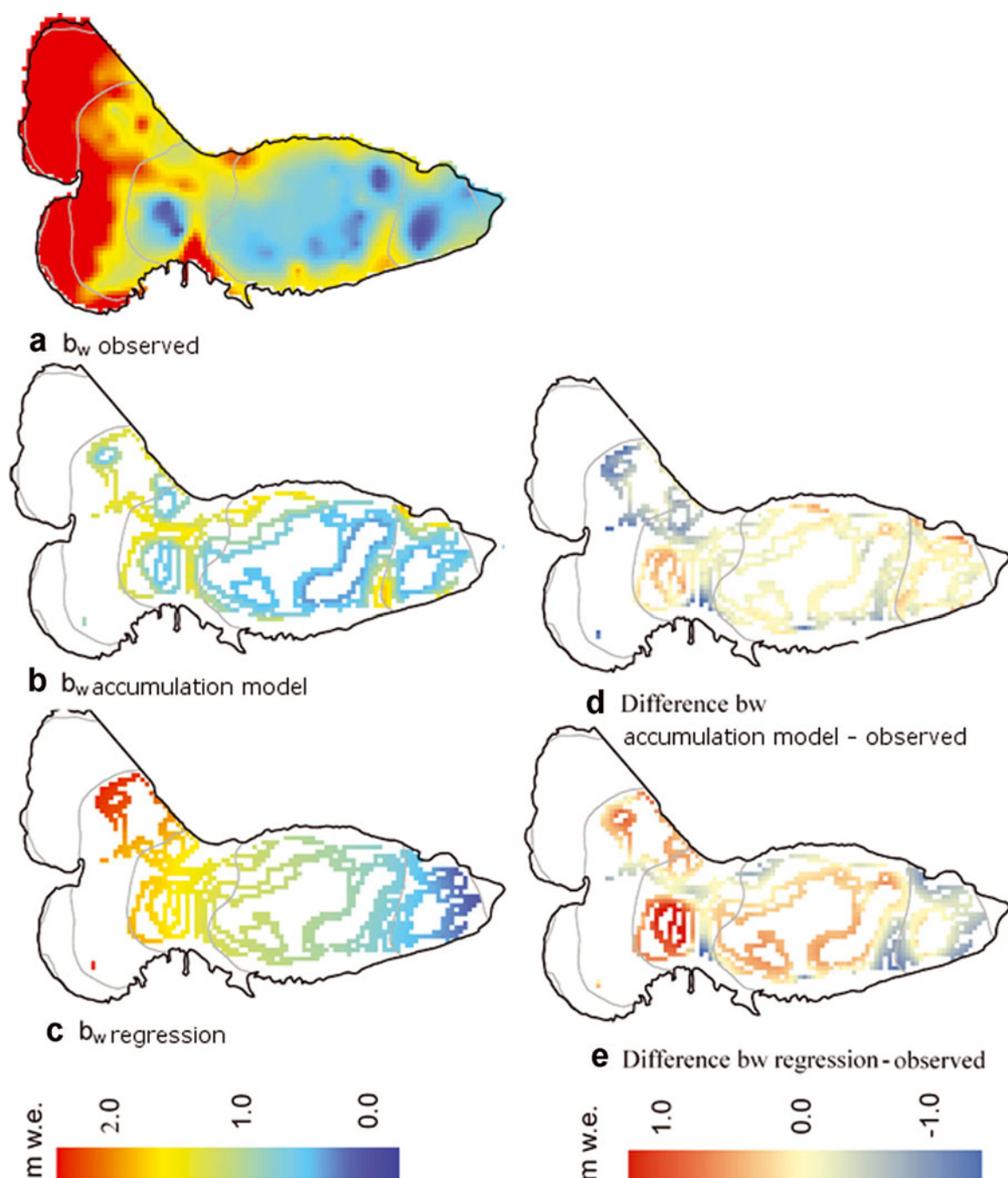


**Fig. 6.** Winter accumulations along tracked snowlines, modelled and observed, and differences (m.w.e.). Grey lines are elevation contours. (a) Observed accumulation grid derived from kriging on 266 measured snow-probing points. (b) Results from the accumulation model. (c) Results from the linear regression model. (d) Difference between the accumulation model and observed winter accumulation. (e) Difference between the regression model and observed winter accumulation.

A limitation of the snow accumulation model is that it only provides estimates of the peak accumulation for the gridcells where we have observations of the transient snowline. However, snowlines are readily accessible from aerial photographs and satellite images for many glaciers around the globe. The recent trend of using time-lapse photography in glaciological studies makes this method even more useful when attempting to retrieve highly detailed snow accumulation estimates of specific glaciers. Even so, interpolation and extrapolation of the accumulation determined at snowlines is required for complete coverage of an accumulation area. Interannual variability of the accuracy of an interpolated accumulation grid is expected,

since it will be dependent on the degree of melt and the spatial distribution and altitude of the snowlines for the specific season. There will also be varying results between glaciers, depending on the hypsometry of the glacier.

## CONCLUSIONS

Snow accumulation data of glaciers are sparse. Field data are expensive and difficult to collect during winter seasons in remote areas, and the spatial distribution of snow accumulation varies locally. The purpose of this study is to develop and assess a method that can represent the spatial snow accumulation distribution and that requires minimum

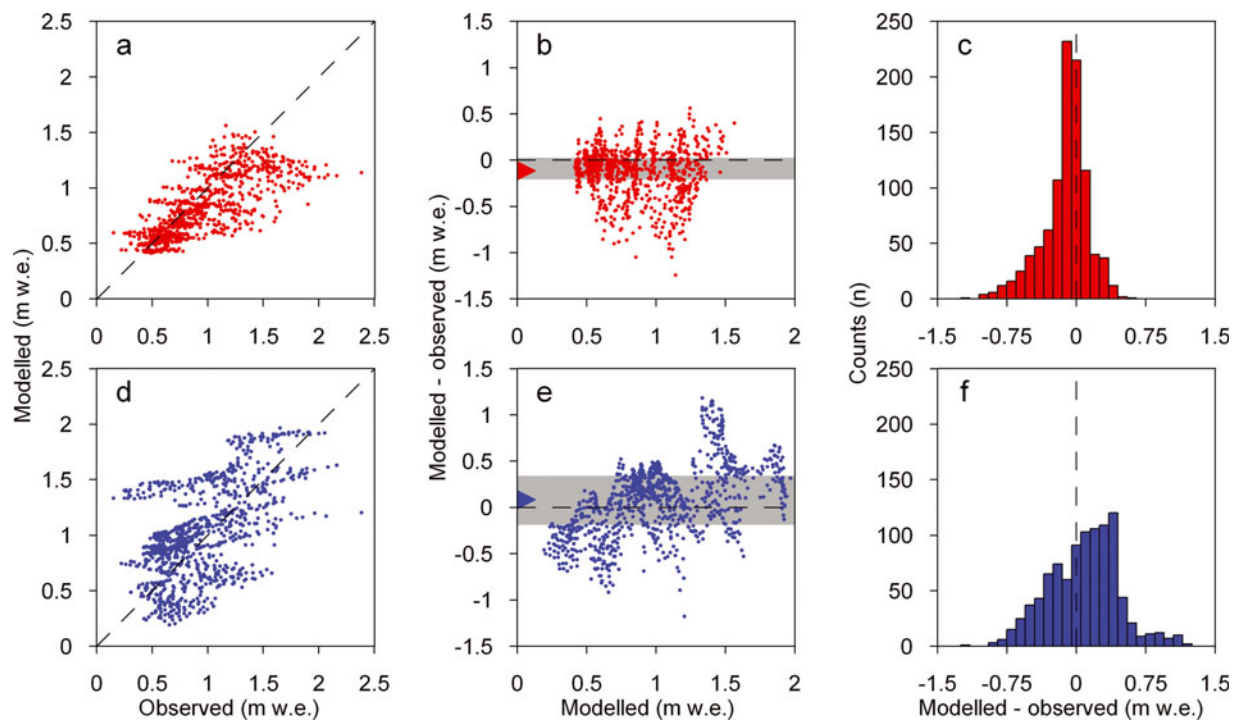


**Fig. 7.** Comparison of observed and modelled accumulation (m w.e.) using the accumulation and regression models at the gridcells along the tracked snowlines. Accumulation model: (a) observed versus modelled; (b) modelled versus difference (modelled – observed); (c) distribution of difference (modelled – observed) versus counts of gridcells ( $n$ ). Regression model: (d) observed versus modelled; (e) modelled versus difference (modelled – observed); (f) distribution of difference (modelled – observed) versus counts of gridcells ( $n$ ). In (b) and (e) the grey regions indicate the interquartile range and the triangles the mean of the model residuals.

input data. In particular, the method can be applied without any available accumulation measurements. A temperature-index melt model is applied backwards (accumulation model), in combination with data on transient snowlines, to determine the winter snow accumulation along the snowlines. The following points have been addressed in this study:

1. On-glacier observations of snowlines during the melt season have been used as a reference point for the accumulation modelling.
2. Observed mean snow accumulation has been derived by interpolating 266 snow-probing points to the snowlines. The interpolated mean snowline accumulation was found to be  $0.94 \pm 0.10$  m w.e. at observed snowlines.
3. A temperature-index melt model has been calibrated using melt measurements from 87 independent stake measurements during the melt season, with a Pearson correlation coefficient of  $R^2 = 0.81$ .
4. The accumulation model, using backward temperature-index melt modelling, has been applied at the snowlines, yielding an average modelled snowline accumulation of  $0.82 \pm 0.25$  m w.e.
5. A linear regression accumulation model based on altitude has been derived using 87 independent accumulation stake measurements, with a Pearson correlation coefficient of  $R^2 = 0.62$ . Application of the regression model at the snowlines yields an average snowline accumulation of  $1.02 \pm 0.38$  m w.e.

**Table 2.** Summary of the statistical assessments presented in the text and figures

	Number of data points	Bias	Pearson correlation coefficient	Standard error
		m	$R^2$	m
Result of melt model calibration using 87 stake melt measurements taken during three different periods (Fig. 3)	103	-0.006	0.81	0.067
Linear regression model for accumulation using 87 stake accumulation measurements (Fig. 5)	87	0	0.62	0.42
Comparison of accumulation model calculations with interpolation of 266 snow probe measurements at snowlines (Fig. 7a)	975	-0.12	0.57	0.25
Comparison of linear regression accumulation model calculations with interpolation of 266 snow probe measurements at snowlines (Fig. 7d)	975	0.08	0.30	0.38

6. The mean deviations between the observed and the modelled snowline accumulation lie within the range of the uncertainty of the measured data but the standard deviation is lower for the accumulation model than for the regression model. This, combined with the higher Pearson correlation coefficient of the accumulation model, indicates that the accumulation modelling method improves the spatial representation of the complex accumulation pattern of Storglaciären.
7. The results also show that information on transient snowline locations can be usefully applied for the determination of the winter snow accumulation.

## ACKNOWLEDGEMENTS

The project was partially funded by the Norwegian University of Life Sciences, ISP (the Norwegian Research Council) and NCoE SVALLI. We thank Tarfala Research Station for providing the meteorological and mass-balance data. D Koostra performed the snowline measurements.

## REFERENCES

- Bagchi AK (1983) Areal value of degree-day factor. *Hydrol. Sci. J.*, **28**(4), 499–511
- Blöschl G, Kirnbauer R and Gutknecht D (1991) Distributed snowmelt simulations in an Alpine catchment. I. Model evaluation on the basis of snow cover patterns. *Water Resour. Res.*, **27**(12), 3171–3179 (doi: 10.1029/91WR02250)
- Cline DW (1997) Snow surface energy exchanges and snowmelt at a continental, midlatitude Alpine site. *Water Resour. Res.*, **33**(4), 689–701 (doi: 10.1029/97WR00026)
- Farinotti D, Magnusson J, Huss M and Bauder A (2010) Snow accumulation distribution inferred from time-lapse photography and simple modelling. *Hydrol. Process.*, **24**(15), 2087–2097 (doi: 10.1002/hyp.7629)
- Gardner AS and Sharp M (2009) Sensitivity of net mass-balance estimates to near-surface temperature lapse rates when employing the degree-day method to estimate glacier melt. *Ann. Glaciol.*, **50**(50), 80–86 (doi: 10.3189/172756409787769663)
- Grudd H and Schneider T (1996) Air temperature at Tarfala Research Station 1946–1995. *Geogr. Ann. A*, **78**(2–3), 115–120
- Hock R (1999) A distributed temperature-index ice- and snowmelt model including potential direct solar radiation. *J. Glaciol.*, **45**(149), 101–111
- Hock R and Holmgren B (2005) A distributed surface energy-balance model for complex topography and its application to Storglaciären, Sweden. *J. Glaciol.*, **51**(172), 25–36 (doi: 10.3189/172756505781829566)
- Hock R, Johansson M, Jansson P and Barring L (2002) Modeling climate conditions required for glacier formation in cirques of the Rassepautasjtjåkka Massif, northern Sweden. *Arct. Antarct. Alp. Res.*, **34**(1), 3–11
- Hock R, Kootstra D-S and Reijmer C (2007) Deriving glacier mass balance from accumulation area ratio on Storglaciären, Sweden. *IAHS Publ.* 318 (Symposium at Foz do Iguaçu 2005 - Glacier Mass Balance Changes and Meltwater Discharge), 163–170
- Holmlund P (1996) Maps of Storglaciären and their use in glacier monitoring studies. *Geogr. Ann. A*, **78**(2–3), 193–196
- Holmlund P and Jansson P (1999) The Tarfala mass-balance programme. *Geogr. Ann. A*, **81**(4), 621–631 (doi: 10.1111/j.0435-3676.1999.00090.x)
- Holmlund P, Jansson P and Pettersson R (2005) A re-analysis of the 58 year mass-balance record of Storglaciären, Sweden. *Ann. Glaciol.*, **42**, 389–394 (doi: 10.3189/172756405781812547)
- Hulth J (2006) Ackumulationsmönster på Storglaciären 1966–2005. (MSc thesis, University of Stockholm)
- Huss M, Bauder A, Werder M, Funk M and Hock R (2007) Glacier-dammed lake outburst events of Gornersee, Switzerland. *J. Glaciol.*, **53**(181), 189–200 (doi: 10.3189/172756507782202784)
- Jansson P (1999) Effect of uncertainties in measured variables on the calculated mass balance of Storglaciären. *Geogr. Ann. A*, **81**(4), 633–642
- Kootstra D-S (2005) Determining glacier mass balance from surrogate variables: a case study on Storglaciären using ELA and AAR. (MSc thesis, University of Stockholm)
- Nash JE and Sutcliffe JV (1970) River flow forecasting through conceptual models. Part 1. A discussion of principles. *J. Hydrol.*, **10**(3), 282–290 (doi: 10.1016/0022-1694(70)90255-6)
- Ohmura A (2001) Physical basis for the temperature-based melt-index method. *J. Appl. Meteorol.*, **40**(4), 753–761 (doi: 10.1175/1520-0450(2001)040<0753:PBFTTB>2.0.CO;2)
- Pellicciotti F, Brock BW, Strasser U, Burlando P, Funk M and Corripio JG (2005) An enhanced temperature-index glacier melt model including shortwave radiation balance: development and testing for Haut Glacier d'Arolla, Switzerland. *J. Glaciol.*, **51**(175), 573–587 (doi: 10.3189/172756505781829124)
- Raleigh MS and Lundquist JD (2009) Calculating snowmelt backwards – using the date of snowpack disappearance to determine how much snow fell over a season. *Am. Geophys. Union, Fall Meet.* [Abstr. C31B-0447]
- Raleigh MS and Lundquist JD (2010) A snow hydrologist's time machine: determining winter snow accumulation with spring-time mass and energy exchanges at the air–snow interface. In *CUAHSI 2nd Biennial Colloquium on Hydrologic Science and Engineering, 19–22 July 2010, Boulder, CO*. [http://www.cuahsi.org/biennial2010/abstracts-posters.html#\\_Toc265224202](http://www.cuahsi.org/biennial2010/abstracts-posters.html#_Toc265224202)
- Rango A and Martinec J (1982) Snow accumulation derived from modified depletion curves of snow coverage. *IAHS Publ.* 138 (Symposium at Exeter 1982 – *Hydrological Aspects of Alpine and High Mountain Areas*), 83–90
- Schuler TV, Melvold K, Hagen JO and Hock R (2005) Assessing the future evolution of meltwater intrusions into a mine below Gruefonna, Svalbard. *Ann. Glaciol.*, **42**, 262–268 (doi: 10.3189/172756405781812970)
- Schuler TV, Loe E, Taurisano A, Eiken T, Hagen JO and Kohler J (2007) Calibrating a surface mass-balance model for Austfonna ice cap, Svalbard. *Ann. Glaciol.*, **46**, 241–248 (doi: 10.3189/172756407782871783)
- Schytt V (1973) Snow densities on Storglaciären in spring and summer. *Geogr. Ann. A*, **55**(3–4), 155–158
- Sicart JE, Wagnon P and Ribstein P (2005) Atmospheric controls of the heat balance of Zongo Glacier (16° S, Bolivia). *J. Geophys. Res.*, **110**(D12), D12106 (doi: 10.1029/2004JD005732)
- Turpin OC, Ferguson RI and Clark CD (1997) Remote sensing of snowline rise as an aid to testing and calibrating a glacier runoff model. *Phys. Chem. Earth*, **22**(3–4), 279–283 (doi: 10.1016/S0079-1946(97)00144-4)
- Williams RS, Jr, Hall DK and Benson CS (1991) Analysis of glacier facies using satellite techniques. *J. Glaciol.*, **37**(125), 120–128
- Zemp M and 6 others (2010) Reanalysis of multi-temporal aerial images of Storglaciären, Sweden (1959–99). Part 2: Comparison of glaciological and volumetric mass balances. *Cryosphere*, **4**(3), 345–357 (doi: 10.5194/tc-4-345-2010)